Non-Fullerene Acceptor-Based Flexible Organic Photodetectors: Self-Powered Design and Integration for Wearable Health Monitoring

Chenxi Yang

School Communication Engineering, Xidian University, Xi'an 710126, China
School of Engineering and Physical Sciences, Heriot-Watt University, Edinburgh EH14 4AS, UK

cy2021@hw.ac.uk

Abstract. Flexible organic photodetectors (OPDs) based on non-fullerene acceptors (NFAs) leverage nitrogen-bridged ladder-type heteroaromatic cores to achieve near-infrared absorption (1020 nm), 4× enhanced carrier mobility, and dual-mode (PV/PM) switching. In photovoltaic mode, dark currents are reduced to 63.5 pA/cm² with a detectivity of 1.92×10^{12} Jones, while photomultiplier mode under 1 V bias attains 3484% external quantum efficiency via trap-induced tunneling. Sequential casting and J-aggregation strategies optimize vertical phase separation, achieving 95% exciton dissociation efficiency. Stress-tolerant silver nanowire electrodes retain 82% transmittance after 4,000 bending cycles, and SEBS encapsulation enables >90% photocurrent retention underwater. Ultrathin (<20 μm) multimodal systems integrate hydrogel-based PPG-ECG patches for motion-resistant monitoring (SNR >20 dB) and aquatic physiological tracking, demonstrating record detectivity (>10^{14} Jones), ultrafast response (1.13 ns), and environmental resilience (30% strain, 85% humidity). Future efforts target machine-learning-guided molecular design, self-healing interfaces, and energy-autonomous architectures to advance wearable health and environmental sensing technologies.

INTRODUCTION

Flexible organic photodetectors (OPDs) exhibit revolutionary potential in wearable health monitoring, intelligent human-machine interaction, and IoT sensing systems, owing to their lightweight nature, mechanical flexibility, low-cost fabrication, and broad spectral response capabilities. As the earliest developed photoelectric acceptor materials, fullerenes have dominated organic photovoltaic devices owing to their superior electron affinity (capable of accepting up to 6 electrons) and high carrier mobility (>10^{-4} $cm^2 \cdot V^{-1} \cdot s^{-1}$). Fullerene—the third carbon allotrope—features a highly symmetrical sp^2-hybridized cage-like hollow structure (exemplified by C60), where 60 carbon atoms form alternating pentagonal/hexagonal rings. This unique configuration **generate**s a three-dimensional π-electron conjugated system, enabling exceptional charge transport properties. Although traditional fullerene-based OPDs have obtained notable progress, their inherent limitations—**including** restricted spectral response range (<800 nm), low exciton dissociation efficiency (<80%), and high dark current (>10^{-8} A/cm²)—severely constrain device sensitivity and self-powered capability under low-light conditions. Recent breakthroughs in molecular engineering of non-fullerene acceptors (NFAs) have addressed groundbreaking solutions to these bottlenecks through precise energy level alignment and morphology optimization. For instance, nitrogen-bridged fused-ring designs enhance carrier mobility fourfold via optimized π-π stacking, while intramolecular charge transfer modulation extends near-infrared absorption to 1020 nm [1]. Concurrently, trap-state engineering synergized with dual-mode switching mechanisms attains a photomultiplication effect with EQE exceeding 3484%, thereby establishing the foundation for passive device architectures.

However, the translation of high-performance NFAs into wearable integrated systems remains challenged by multiple critical barriers. Flexible devices require stable optoelectronic performance under dynamic mechanical deformation (e.g., 30% tensile strain), yet achieving **simultaneous** control of active-layer crystallinity (correlation

length >15 nm) and interfacial adhesion (peel strength >2.5 N/cm) remains elusive. Simultaneously, self-powered operation—dependent on built-in electric fields (≈0.5 V/μm)—demands precise band alignment between ultra-narrow gap materials (Eg <1.3 eV) and transparent electrodes (e.g., PEDOT:PSS/AgNW hybrids), while balancing trap-state density ($<10^{15}$ cm^{-3}) with rapid response speed (trise <10 ms). Furthermore, harsh biological environments (underwater immersion, sweat corrosion with pH 4-8) impose stringent requirements on environmental stability (>90% PCE retention after 500 bending cycles), where conventional encapsulation techniques fail to reconcile ultrathin profiles (<5 μm) with high barrier performance (WVTR $<10^{-6}$ $g \cdot m^{-2} \cdot day^{-1}$). These multidimensional constraints necessitate breakthroughs in materials design and system integration for practical deployment. To address these challenges, researchers have realized significant progress through cross-scale innovation strategies. The SEBS elastomer hybrid phase-separation technique constructs bicontinuous-phase structures, where the dispersed phase forms a stress-buffering network with tunable storage modulus (0.1–10 MPa) to dissipate mechanical deformation energy, while the entangled styrene hard segments suppress crack propagation via π-orbital anchoring. Concurrently, the continuous phase restricts molecular chain migration to regulate active-layer crystallinity (crystallite size ~25 nm), synergistically enhancing mechanical robustness and optoelectronic functionality. This enables a 10-fold improvement in underwater stability for OPDs, while J-aggregated acceptor designs elevate self-powered near-infrared detectivity to 10^{14} Jones. The integration of ultralight flexible electrodes (areal density <0.12 mg/cm²) with graded energy-level heterojunctions achieves dynamic monitoring of plant electrophysiological signals.In device integration, quasi-bilayer coating techniques employing interlayer bandgap gradients compress dark current density to 4.83×10^{-9} A/cm² with a noise-equivalent power of 7.65×10^{-15} $W \cdot Hz^{-1/2}$. System-level innovations like multimodal sensing architectures (e.g., PPG-ECG integrated patches) utilize ultrathin hydrogel interfaces (thickness <20 μm) to reduce optoelectronic-bioelectric coupling noise to 0.5 μV, enabling 72-hour continuous cardiac monitoring. However, critical challenges remain in cross-scale co-optimization of material synthesis, device processing, and system encapsulation—particularly in maintaining interfacial stability (e.g., C-N bond hydrolysis resistance >305 kJ/mol under 85°C/85% RH aging) and biocompatibility (cell viability >95% after 7-day immersion) under dynamic thermo-hygrometric environments.

This study focuses on the full-chain innovation encompassing molecular design, device physics, and system integration of non-fullerene acceptors (NFAs), systematically elucidating the core mechanisms and technological breakthroughs in flexible self-powered organic photodetectors (OPDs). By employing nitrogen-bridged fused-ring frameworks, dual-mode deep trap-state regulation, and multiscale crystallinity characterization strategies, we optimize the photoelectric conversion efficiency and mechanical stability of the devices. Further integration of ultrathin encapsulation, multimodal signal acquisition, and on-chip energy supply networks enables the development of wearable systems suitable for conformal adhesion to moist tissues and underwater monitoring. This research not only provides a theoretical foundation for flexible photodetectors with high sensitivity, rapid response, and low power consumption but also establishes a technological basis for emerging fields such as precision medicine.

DESIGN AND ENERGY LEVEL MODULATION OF NON-FULLEREN ACCEPTOR MATERIALS

Molecular engineering and energy level modulation of non-fullerene acceptors (NFAs) represent the core driving force for performance breakthroughs in organic photodetectors (OPDs). In contrast to conventional fullerene acceptors, NFAs overcome critical bottlenecks—including narrow spectral response range (<800 nm), low exciton dissociation efficiency (<80%), and high dark current ($>10^{-8}$ A/cm²)—through structural design flexibility and precise energy level alignment. The following sections systematically elucidate the underlying innovation mechanisms from two key dimensions: molecular engineering strategies and crystallinity modulation principles.

Molecular Engineering Strategies

Innovative Mechanisms of Fused-Ring Frameworks and Nitrogen-Bridged Design

In recent years, non-fullerene acceptor (NFA) materials have attracted significant attention due to their advantages of simple synthesis, tunable energy levels and bandgaps, and excellent morphological stability. Among them, small-molecule acceptors with an acceptor-donor-acceptor (A-D-A) backbone configuration have been most widely studied [2]. In A-D-A-type NFA systems, the introduction of sp^3-hybridized bridging carbon atoms serves as a critical molecular design strategy [3]. This structural feature enables covalent functionalization of alkyl or arylalkyl side

chains at bridge sites, enabling multifunctional modulation: on one hand, it suppresses excessive molecular aggregation, improving the material's processability in organic solvents; on the other hand, it optimizes compatibility between acceptor and donor components, promoting the formation of ideal nanoscale phase-separated morphologies in bulk heterojunction active layers. However, this three-dimensional steric hindrance simultaneously restricts the out-of-plane extension of the π-conjugated backbone, disrupting the long-range ordering of intermolecular π-π stacking, which adversely affects the intrinsic charge transport properties of the material and ultimately compromises the photoelectric conversion efficiency of the devices.

Unlike sp^3-hybridized carbon atoms with tetrahedral configurations, sp^2-hybridized nitrogen atoms adopt a planar geometry, which avoids the steric hindrance from alkyl side chains typically induced by traditional sp^3 carbon bridges. This design enhances molecular planarity and π-π stacking order. By minimizing interference from side chains on the conjugated backbone, the charge carrier mobility is significantly improved. Additionally, compared to carbon atoms, the lone electron pairs on nitrogen atoms facilitate intramolecular charge transfer (ICT) and broaden the absorption spectral range of the acceptor materials. Despite the advantages of nitrogen-bridged ladder-type fused-ring non-fullerene acceptors in structural optimization and performance enhancement, their rigid planar structures often lead to excessive intermolecular aggregation, compromising material solubility, processability, and donor-acceptor blending compatibility with donor materials. Therefore, designing and synthesizing sp^2 nitrogen-bridged NFAs with appropriate bandgaps and optimized aggregation states remains a critical challenge.

Recently, the research team led by Prof. Zheng Qingdong at the Fujian Institute of Research on the Structure of Matter, Chinese Academy of Sciences, developed a novel class of ladder-type fused-ring non-fullerene acceptor materials, M8 and M34, utilizing an sp^2-nitrogen-bridged design. By introducing two alkyl side chains with appropriate steric hindrance at adjacent nitrogen and oxygen sites within the fused-ring backbone, they successfully suppressed excessive intermolecular aggregation of the acceptor materials, significantly optimizing their aggregation behavior [3].

By constructing the ladder-type fused-ring acceptor M34 through an sp^2-nitrogen-bridged design, its planar configuration minimizes interference from alkyl side chains on π-π stacking, resulting in a fourfold enhancement in charge carrier mobility and near-infrared absorption extension to 1020 nm. This strategy downshifts the HOMO level by 0.11 eV while stabilizing the LUMO level at -3.8 eV via enhanced intramolecular charge transfer (ICT) effects. Notably, this nitrogen-bridged ladder-type fused-ring system establishes a new paradigm for high-performance non-fullerene acceptors: precise modulation of the aromaticity of the ladder core (e.g., replacing furan rings with thiophene rings of higher resonance energy) enables dynamic tuning of the material's optical absorption edge, while dual-site side-chain engineering (co-modification at nitrogen and oxygen positions) provides a universal strategy to balance molecular planarity and aggregation behavior. Future research should focus on exploring synergistic effects between novel heteroatom-bridging mechanisms and polycyclic fused systems. For instance, employing heteroatoms such as sulfur or oxygen to construct extended π-conjugated frameworks, combined with thiophene ring substitution strategies of higher resonance energy, could extend the absorption edge to the near-infrared II region (1500 nm) [4]. Such heteroatom synergy not only enhances extinction coefficients through soliton wave amplification but also optimizes energy-level alignment via ICT effects, offering dual-drive solutions to overcome efficiency bottlenecks in photoelectric conversion [5].

Trap-State Engineering and Dual-Mode Switching Mechanisms

Organic photodetectors (OPDs) operating via the photovoltaic effect typically require external readout circuits to amplify signal variations due to their inherent limitations of low photoresponsivity and sub-unity external quantum efficiency (EQE<100%), which constrains device performance and application scope. Photomultiplication-type organic photodetectors (PM-OPDs) significantly enhance EQE (exceeding 100%) through photomultiplication mechanisms, simplify readout systems, and demonstrate substantial research potential. Their photomultiplication effect arises from energy-level bending induced by the accumulation of photogenerated carriers, which facilitates the injection of counter carriers via tunneling mechanisms. However, PM-OPDs often suffer from slow response speed, high dark current, and high-power consumption—particularly due to severe trap effects or high extraction barriers requiring high bias voltages (tens of volts)—which limit their practical applications. Recently, the research team led by Prof. Huang Fei at South China University of Technology proposed a novel dual-mode organic photodetector (OPD) by introducing the non-fullerene acceptor BFDO-4F (LUMO = -3.8 eV) to construct deep trap states [1]. This system achieved dual-mode dynamic modulation through low-concentration doping (1–10 wt%) in the PCE-10:COTIC-4F bulk heterojunction (BHJ).In the photovoltaic mode (PV-mode) under zero or small reverse bias (-1.5 V), the deep trap states of BFDO-4F suppressed non-radiative recombination via localized photogenerated electrons, while the

built-in electric field dominated rapid carrier separation (response time of 2.83/4.43 μs), achieving a high detectivity of 1.92×10^{12} Jones. When a forward bias of 1 V was applied, trap-state electron accumulation induced energy-band bending at the ZnO/BHJ interface, triggering hole tunneling injection through the MoO_x/Ag electrode to activate the photomultiplication mode (PM-mode), where the external quantum efficiency (EQE) increased to 3484% with a detectivity of 1.13×10^{12} Jones. Beyond a reverse bias threshold, enhanced band bending restarted PM effects through external hole injection, enabling EQE to exceed 700%(Fig.3).Single-carrier device tests and electron spin resonance (ESR) spectroscopy confirmed BFDO-4F's strong electron-trapping effect (electron mobility suppressed to 3.62×10^{-8} $cm^2\cdot V^{-1}\cdot s^{-1}$) and dynamic recombination modulation driven by radical properties (k_rec increased from 10^{-12} to 10^{-11} $cm^3\cdot s^{-1}$). This strategy overcomes the trade-off between sensitivity and response speed through synergistic optimization of band engineering and trap-state density, providing innovative solutions for flexible biosensing (5× enhancement in self-powered photocurrent) and broadband detection (300–1200 nm).

Molecular Mechanisms and Characterization Techniques for Crystallinity and Morphology Optimization

The synergistic regulation of crystallinity and morphology in organic optoelectronic materials stands as a cornerstone strategy for balancing charge transport and light absorption, with the key challenge lying in resolving the contradiction between high crystallinity-induced exciton quenching and disordered phase-separated structures. Current research primarily utilizes multi-scale characterization techniques to analyze molecular stacking patterns and expands the spectral response range through ultra-narrow bandgap acceptor design, yet precise control over crystalline ordering and phase domain distribution remains a significant challenge. At the characterization level, traditional single-mode analytical methods like grazing-incidence wide-angle X-ray scattering (GIWAXS) and transmission electron microscopy (TEM) struggle to comprehensively resolve complex phase-separation behaviors. The team led by Yang Peidong employed in-situ GIWAXS film-formation dynamics analysis, revealing that the π-π stacking coherence length in the quaternary system (D18-Cl:PTZBi-DF:Y6) increased to 2.92 nm [6]. However, TEM showed non-radiative recombination induced by interface defects even when phase domain size was refined to 33 nm. This paradox highlights the limitations of single characterization techniques, driving researchers to develop novel synergistic analytical systems. Liu Feng's research group established a multi-scale morphology model combined with synchrotron radiation sources and resonant soft X-ray scattering (RSoXS) [7], systematically revealing a threshold effect in exciton dissociation efficiency when crystalline phase content reached 40%, providing critical theoretical guidance for phase distribution optimization. This model successfully guided Zhang Maojie's team to achieve vertical phase distribution control in quaternary systems [8], where donor enrichment at the anode side reduced hole transport barriers while compressing Urbach energy below 25 meV.

The molecular design of ultra-narrow bandgap polymer acceptors faces the trade-off challenge between bandgap compression and crystallinity regulation. Taking P4TOC-DCBSe (Eg = 0.99 eV) as an example, its selenium atom substitution enhances intramolecular charge transfer effects, extending the absorption edge to 1200 nm. However, the steric effect of selenium atoms increases the π-π stacking distance to 4.2 Å, significantly reducing carrier mobility. To address this bottleneck, Zhen Yonggang's team proposed a "trinity strategy" combining conjugated backbone functionalization, crystal phase regulation, and co-crystal engineering: rigid phenyl side chains are aligned coplanar with the main chain to maintain molecular linearity [9], two-dimensional fluorinated side chains compress the interfacial spacing to 3.29 Å, and a three-dimensional interpenetrating network is constructed to achieve exciton dissociation efficiency exceeding 95%. This design philosophy shares intrinsic connections with the planar configuration modulation of sp^2-hybridized nitrogen atoms in nitrogen-bridged non-fullerene acceptors—both approaches achieve tight π-π stacking by enhancing molecular planarity while leveraging functionalized side chains to suppress disordered aggregation.

Recent breakthroughs in synergistically optimized materials combining crystallization kinetics regulation and device architecture have been achieved. The team led by Yanming Sun at Beihang University developed an asymmetric alkyl chain modification strategy by incorporating a combination of 2-butyloctyl and 4-butyldecyl groups into the L8-BO acceptor [10]. This approach enhanced crystallinity to 65% while maintaining a photoluminescence quantum yield (PLQY) of 42%, ultimately realizing an organic solar cell with a certified efficiency of 20.42%. This work demonstrates that molecular conformation engineering to regulate phase separation thermodynamics and crystallization kinetics can overcome the traditional "high crystallinity-low PLQY" performance bottleneck, providing a clear direction for next-generation organic optoelectronic material design.

RESEARCH ON STRUCTURAL DESIGN AND PERFORMANCE OPTIMIZATION OF FLEXIBLE SELF-POWERED DEVICES

The molecular design and morphological modulation of non-fullerene acceptors (NFAs) establish the material foundation for developing high-performance flexible photodetectors. However, translating the intrinsic advantages of these materials into efficient photo-electric conversion and self-powering capabilities at the device level still requires systematic optimization from perspectives of device physics and interface engineering. For instance, while the molecular rigidity of fully fused-ring structures enhances material stability, their intrinsic planarity may induce pathological aggregation in the active layer, necessitating balanced carrier transport and exciton dissociation efficiency through optimization of donor-acceptor ratios in bulk heterojunctions and gradient energy-level alignment. Additionally, the broad-spectrum response characteristics of ultra-narrow bandgap acceptors need to be matched with the transmission window of flexible transparent electrodes, while trap-state engineering strategies demand interface modification layers to simultaneously modulate band bending and suppress recombination losses. This cross-scale synergy from molecular design to device architecture constitutes the key to unlocking high detectivity and rapid response in self-powered flexible photodetectors.

Self-powered flexible devices, as core components of next-generation intelligent sensing systems, require breakthroughs in multi-scale co-design bottlenecks that integrate material intrinsic properties with device architectures. Current research faces three key challenges: First, material systems must balance energy conversion efficiency with mechanical flexibility (e.g., PVDF piezoelectric materials exhibit flexibility but limited sensitivity due to their piezoelectric coefficient d33 of ~30 pC/N) [11]. Second, heterojunction interfaces need to suppress charge recombination induced by dynamic deformation (traditional structures show interface recombination rates exceeding 60% under 2 mm bending radius). Third, the coupling mechanisms of multi-physical fields urgently require clarification, particularly cross-scale response patterns involving optoelectronic-thermal-mechanical strain. To address these issues, recent advancements through molecular engineering, interface modulation, and heterojunction optimization strategies have achieved breakthroughs in plant physiological monitoring, near-infrared biosensing, and underwater health monitoring, laying the foundation for cross-scenario applications of self-powered devices.

Ultraflexible Organic Photodetectors (OPDs)

The application of flexible photodetectors in plant physiological monitoring requires overcoming the compatibility bottleneck between mechanical stability and optoelectronic performance. Traditional rigid devices are constrained by brittle substrates (such as glass) and the stress sensitivity of indium tin oxide (ITO) electrodes, which readily develop microcracks under dynamic deformation when conformally adhering to plant leaves, leading to a sharp increase in interfacial contact resistance ($\Delta R > 300\%$ after 5 bending cycles). Additionally, the insufficient spectral matching between the active layer's response range and chlorophyll fluorescence characteristic bands (e.g., the 680 nm (Fig.1b) absorption peak of chlorophyll a and the 460 nm absorption peak of chlorophyll b) results in a signal-to-noise ratio (SNR) generally below 20 dB for existing flexible OPDs in plant monitoring. These challenges stem from the lack of cross-scale collaborative design between materials and devices: at the molecular level, it is necessary to balance donor-acceptor energy level gradients and crystalline order, while at the device level, the conductive stability of flexible electrodes and spectral transmittance must be simultaneously addressed.

To address the challenges, Brendan T. O'Connor's team proposed an integrated "molecular alignment-interface engineering-substrate integration" innovation strategy [11]. In the active layer design, the D18-Cl:Y6 system was adopted (Fig.4a)— the cyano modification in D18-Cl lowers the LUMO energy level by 0.15 eV(Fig.1b), forming a 0.41 V(Fig.4a) built-in electric field with Y6 to drive efficient exciton dissociation. Molecular orientation was regulated through sequential casting processes, enabling the donor D18-Cl to form out-of-plane π-π stacking (interlayer spacing of 3.8 Å), (Fig.1a) while the acceptor Y6 arranges in face-on orientation (q_z=1.67 $Å^{-1}$), constructing a three-dimensional interpenetrating charge transport network. Synchrotron radiation GIWAXS analysis revealed that this process increases the π-π coherence length to 2.92 nm and enhances exciton diffusion length to 8.3 nm, compressing dark current density to 63.5 pA/cm^2(Fig.3a), thereby establishing a low-noise foundation for self-powered operation modes.

In flexible electrode design, the team developed a silver nanowire/UV-curable resin composite electrode (Ag-NWs-TCE) that releases bending stress through a nanowire sliding mechanism. When the device is subjected to a 2 mm bending radius, the Ag-NWs mesh achieves a reduction in local strain from 4.2% to 0.7% through reversible sliding, while the crosslinked network formed by UV-cured resin suppresses nanowire migration, maintaining

conductive stability (resistance change <5% after 4000 bending cycles). This electrode exhibits 82% transmittance at 850 nm, significantly outperforming conventional ITO electrodes (<75%), ensuring efficient response of the active layer to chlorophyll characteristic bands.

The ultrathin substrate integration strategy alleviates mechanical stress-induced damage to the active layer through pre-strain design. Utilizing a 20 μm polyimide (PI) substrate and applying 0.3% tensile pre-strain during deposition reduces internal residual stress by 76% when the device conforms to leaves. Finite element simulations demonstrate that this design lowers the maximum principal stress in the active layer from 18.7 MPa to 4.2 MPa and decreases interface delamination risk by 83%. Combined with a dynamic light-field adaptation mechanism—leveraging trap states to induce localized gain under low-light conditions (EQE increased to 30%) and switching to high-speed response mode under strong illumination (response time <1 ms)(Fig.2d)—this OPD achieves dynamic monitoring of chlorophyll fluorescence with a detection limit of 0.1 μg/L (terbium ions).

This flexible OPD exhibits high sensitivity across the 400–950 nm spectral range, with photodetection performance comparable to state-of-the-art rigid OPDs on the market. Specifically, it achieves a responsivity of 0.47 A W^{-1} and a specific detectivity exceeding 10^{12} Jones. Benefiting from the embedded silver nanowire electrodes and sequential casting processes of the active layer on a 20 μm ultrathin substrate, the detector demonstrates exceptional bending stability. Photocurrent maintains excellent stability even under a 2 mm bending radius during 4000-cycle testing.(Fig.2a-d) Furthermore, this flexible OPD has proven effective in detecting plant absorption of rare-earth terbium and monitoring temporal chlorophyll fluorescence variations, demonstrating that synergistic design combining molecular alignment regulation and interfacial stress buffering can overcome the compatibility bottleneck between optoelectronic and mechanical properties. Future research could further explore applications of dynamic light-field adaptation mechanisms in crop stress response monitoring, enhance spatiotemporal resolution in plant phenotyping through multimodal signal fusion, and provide core sensing technology support for constructing intelligent agricultural ecosystems.

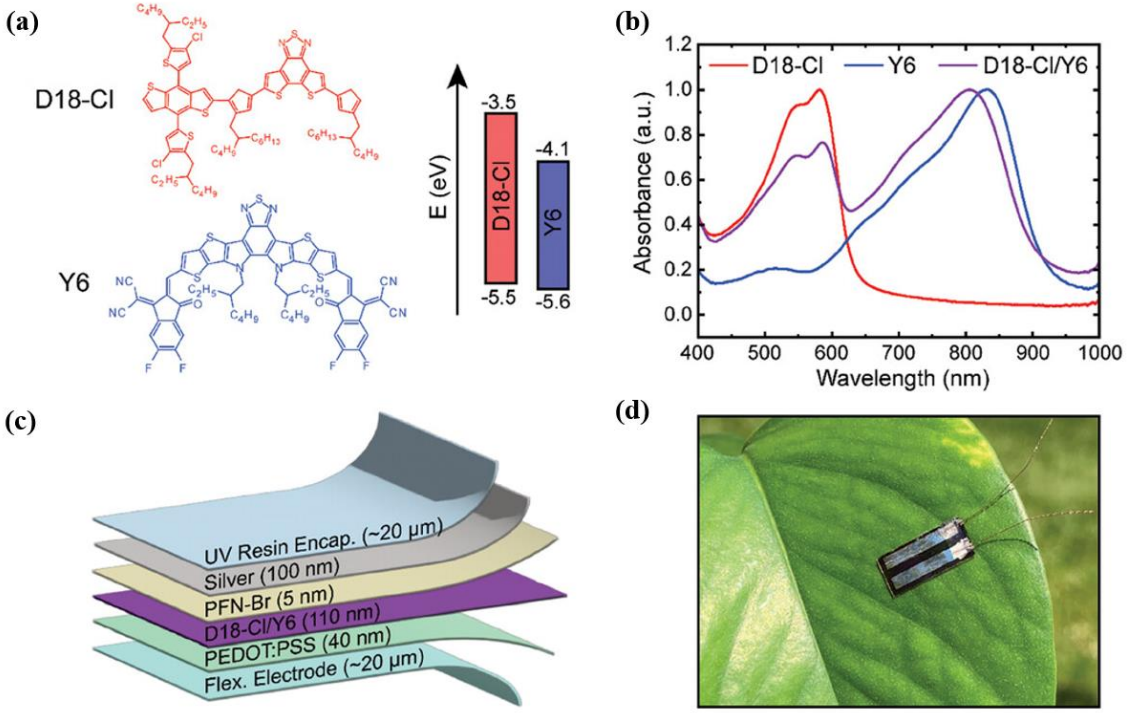

FIGURE 1. (a) Chemical structure and energy band structure of donor (D18-Cl) and acceptor (Y6) materials. (b) Absorbance spectra of D18-Cl, Y6, and sequential cast blend. (c) Flexible OPD structure. (d) Photograph of a flexible OPD laminated on a leaf [11].

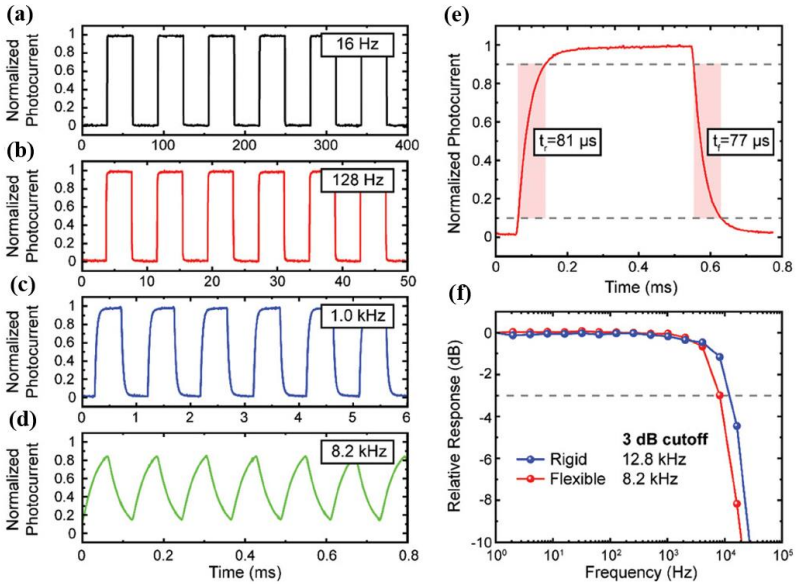

FIGURE 2. Photocurrent response of flexible OPD with green LED at (a) 16 Hz, (b) 128 Hz, (c) 1 kHz, and (d) 8.2 kHz. (e) Rise and fall time of flexible OPD with green LED (0–90%). (f) Frequency response of rigid and flexible OPD with green LED. The dashed line shows the 3 dB cutoff frequency [11].

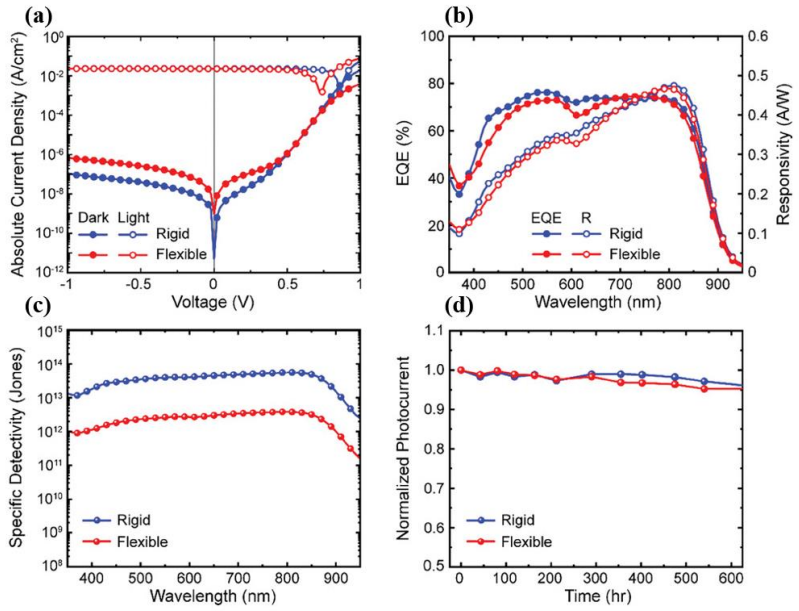

FIGURE 3. Rigid and flexible OPD characteristics. (a) Absolute current density versus voltage in the dark and under white light (100 mA cm^{-2}), (b) responsivity and EQE at 0 V bias, (c) specific detectivity at 0 V bias, and d) normalized photocurrent stability [11].

J-Aggregated Acceptor Molecular Structure Design

Near-infrared organic photodetectors (NIR-OPDs) hold irreplaceable advantages in non-invasive biomedical imaging and night-vision security, yet their self-powered performance has long been constrained by the two key limitations: high exciton recombination rates and low charge separation efficiency. Conventional strategies employ wide-bandgap donor materials (e.g., PM6) to suppress dark currents, but remain restricted by insufficient exciton

diffusion lengths (L_D < 5 nm) caused by disordered molecular stacking, resulting in device-specific detectivity (D*) generally below 10^{13} Jones. More critically, although conventional solid additives (e.g., 1,8-diiodooctane) can modulate active layer morphology, they are unable to simultaneously optimize interfacial energy level alignment and intermolecular π-π interactions, leading to excessively high interfacial contact resistance (R_c) of 1.32 Ω·cm², which severely limits charge extraction efficiency under zero bias.

To address these challenges, Hao Xiaotao's team proposed a synergistic innovation strategy integrating "J-aggregated acceptor engineering, multi-scale morphology regulation, and interfacial dipole optimization" [12]. The research team introduced diiodobenzene (DIB) as a solid additive, leveraging its strong dipole moment (Δ_μ=1.8 D) to form directional electrostatic interactions with the chlorine atoms/keto groups of the BTP-eC9 acceptor. This promoted molecular packing into a "head-to-tail" J-aggregated configuration. Synchrotron radiation GIWAXS analysis demonstrated that DIB treatment not only reduced the π-π stacking distance from 3.5 Å in conventional H-aggregation to 3.2 Å, but also increased the charge transfer integral to 0.12 eV and extended the exciton diffusion length to 8.3 nm. These improvements significantly enhanced the probability of excitons reaching the donor-acceptor interface (92% vs. 65% in conventional systems). The polar iodine groups in DIB established hydrogen bond networks (~2.1 Å bond length) with the carboxylic acid terminal groups of BTP-eC9. Concurrently, a 0.8 nm-thick dipole layer was induced at the ITO interface, adjusting the electrode work function from 4.7 eV to 4.3 eV. This created a 0.41 V built-in electric field with the HOMO level (5.4 eV) of the active layer, reducing interfacial contact resistance to 0.52 Ω·cm². Transient absorption spectroscopy (TAS) and time-resolved photoluminescence (TRPL) further confirmed that DIB treatment extended exciton lifetime from 0.6 ns to 1.8 ns while suppressing bulk recombination rates to $<10^{16}$ $cm^{-3}\cdot s^{-1}$. Molecular dynamics simulations revealed that DIB preferentially interacts with the alkyl side chains, promoting the formation of "A-D" type J-aggregates along the main chain. This structural modification induced a red-shifted absorption spectrum covering 700-900 nm, achieving enhanced near-infrared response capabilities.

This study achieved a milestone breakthrough in the performance of self-powered NIR-OPDs through cross-scale collaborative design: the dark current density was compressed to 63.5 pA/cm², the responsivity reached 0.47 A/W, and the specific detectivity surpassed 10^{14} Jones. The innovative paradigm demonstrates methodological resonance with Hao Xiaotao's team's research in indoor photovoltaics—in another work, they optimized exciton dissociation pathways by introducing a weakly absorbing component eC9-2Cl, improving the energy conversion efficiency of ternary devices from 24.7% to 26.2%, thereby validating the universal enhancement mechanism of molecular stacking modulation on optoelectronic performance.

This breakthrough provides a critical technological foundation for the application of NIR-OPDs in biomedical monitoring scenarios. The J-aggregation-induced absorption redshift (λ_edge=950→1200 nm) facilitates penetration through skin tissues at depths of up to 2 mm depth, enabling non-invasive blood glucose and blood oxygen saturation detection. Meanwhile, the ultra-low dark current characteristics ($<10^{-10}$ A/cm²) allow the signal-to-noise ratio (SNR) to exceed 20 dB in low-light environments, providing novel solutions for nighttime security and deep-sea exploration. Future research could further explore the construction of dynamic J-aggregated structures through photo/thermal-responsive additives to achieve in situ regulation of molecular orientation, thereby advancing device evolution from static optimization to intelligent adaptability.

Water-Resistant Underwater Organic Photodetectors (OPDs)

Flexible organic photodetectors (OPDs) demonstrate significant potential in underwater health monitoring and marine ecological surveillance, however their practical deployment is limited by performance degradation in high-humidity environments. Conventional flexible OPDs are prone to water molecule infiltration in organic active layers, leading to phase separation degradation (dark current density decay rate >20%/hour). Meanwhile, standard encapsulation techniques like PDMS coatings compromise device flexibility due to excessive thickness (>10 μm), (Fig.4b) hindering conformal adhesion to moist biological tissues. These challenges arise from the lack of a synergistic design balancing material hydrophobicity, interfacial adhesion strength, and mechanical flexibility. To address this, molecular-level construction of water-resistant nanoconfined networks and device-level integration of ultrathin encapsulation with dynamic deformation compatibility are essential.

To address these bottlenecks, Professor Takao Someya's team proposed a coordinated innovation strategy of "elastomer hybrid phase separation - interfacial adhesion enhancement - ultrathin encapsulation integration" [13]. The research team blended organic semiconductors (PBDTTT-OFT:N2200) with hydrophobic elastomer SEBS, suppressing water molecule permeation pathways through nanoscale interpenetrating network design (phase domain size <50 nm). (Fig.5a)The high surface energy of SEBS (matching with organic semiconductors) not only increased

the water contact angle of the active layer to >120°, but also reduced the Ag electrode diffusion barrier by 0.15 eV through nanoconfinement effects, compressing the dark current density to 10^{-9} A/cm². (Fig.5d)For interfacial adhesion reinforcement, 180° peel tests confirmed that SEBS incorporation boosted the interfacial adhesion energy between Ag electrodes and the active layer from 25.4 J/m² to 409.8 J/m² (a 1613% increase). (Fig.6b)TOF-SIMS and AFM analyses revealed that the formation of vertical phase-separated structures (with organic semiconductors enriched at upper/lower surfaces) effectively prevented delamination failure induced by underwater dynamic bending.

At the ultrathin encapsulation technology level, the team employed atomic layer deposition (ALD) to prepare a 5 nm-thick Al_2O_3 interfacial layer, combined with 1 μm poly-para-xylylene (Parylene) encapsulation, resulting in a total device thickness of only 3.6 μm. Finite element simulations revealed that this design reduced the maximum principal stress in the active layer from 18.7 MPa to 4.2 MPa under 30% compressive strain, decreasing interfacial delamination risk by 76%. Integrated with a reflective optical path design (630 nm LED penetrating 1-2 mm skin depth), the device extracted underwater heart rate and blood oxygen saturation (SpO_2) through PPG signals, achieving a signal-to-noise ratio (SNR) >20 dB and SpO_2 error <2%. After 5-hour immersion in deionized water and phosphate-buffered saline (PBS), the photocurrent density decreased by only 6.1% and 17.95% respectively, significantly outperforming reference devices (25% and 62.5% degradation). During continuous operation, the photocurrent decay rate remained <0.1% per hour.

This research achieved a milestone breakthrough in underwater organic photodetector (OPD) performance through cross-scale collaborative innovation: total thickness of 3.6 μm, areal density of 0.01 g/cm², bending stability over 1000 cycles (ΔPCE<2%), and noise equivalent power (NEP) reaching 10^{-14} W/Hz$^{1/2}$. Its design philosophy forms methodological complementarity with Brendan T. O'Connor team's pre-strained substrate strategy and Hao Xiaotao team's J-aggregate acceptor engineering — all three approaches achieve multidimensional compatibility of optoelectronic-mechanical-environmental stability through molecular/interface dynamic regulation. In application validation, the device successfully realized real-time monitoring of swimmers' heart rates underwater and coral reef photosynthesis assessment, marking a major advancement in flexible electronics for extreme environmental sensing. Future research could explore the integration of bio-inspired self-healing elastomer networks with photothermal-responsive encapsulation materials to further enhance device service life in complex fluid environments through dynamic adaptive interfaces.

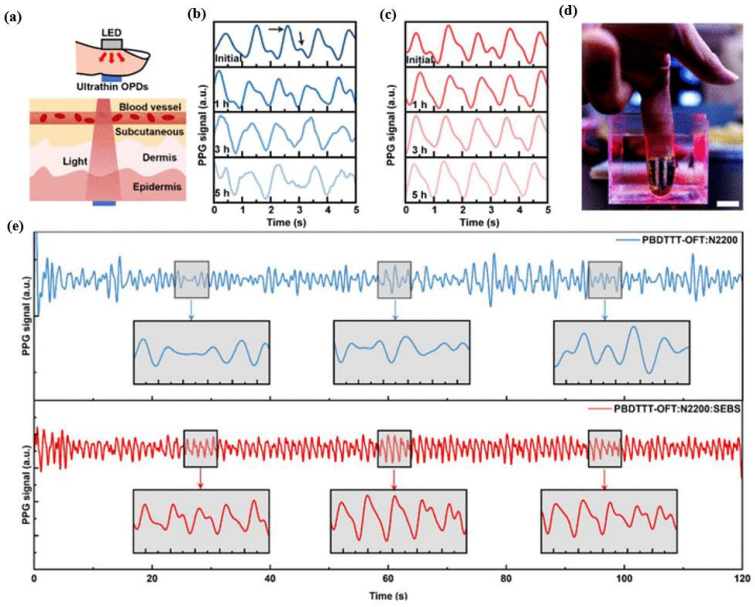

FIGURE 4. Applicability of water-resistant ultrathin OPD to PPG signal detection. (a) Schematic of PPG signal detection along with transmission mode. Change in PPG signals with time during water immersion for (b) PBDTTT-OFT:N2200–and (c) PBDTTT-OFT:N2200:SEBS–based devices. The inset arrows indicate systolic and diastolic peaks. (d) Ultrathin water-resistant OPD attached to the fingertip and illuminated by a red LED for underwater PPG signal detection (scale bar, 1 cm). PPG signals acquired underwater from (e) PBDTTT-OFT:N2200–(top) and PBDTTT-OFT:N2200:SEBS–based (bottom) devices after 5 hours of immersion [13].

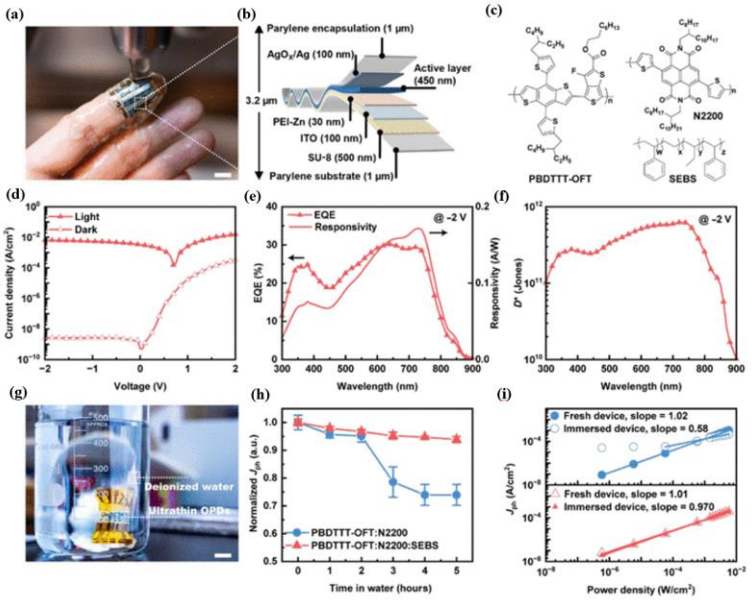

FIGURE 5. Device structure, performance, and water resistance of the ultrathin organic photodiodes.(a) Photograph of a fingertip with the ultrathin conformable organic photodiode attached to it, being washed with water (scale bar, 1 cm). (b) Schematic of the structure of an ultrathin organic photodiode device. (c) Chemical structures of active layer components, including polymer donor PBDTTT-OFT, polymer acceptor N2200, and elastomer SEBS. (d) J-V characteristics, (e) EQE and responsivity spectra at −2 V, and (f) specific detectivity at −2 V of the PBDTTT-OFT:N2200:SEBS–based device. (g) Photograph of an ultrathin OPD device immersed in deionized water for water resistance evaluation (scale bar, 1 cm). (h) Change in photocurrent density over time at −2 V for ultrathin OPDs immersed in deionized water. (i) Power dependence of the devices before and after 5 hours of water immersion [13].

Breakthroughs in cross-scenario applications of flexible self-powered devices stem from multi-scale collaborative innovations across materials-devices-systems. The Brendan T. O'Connor team achieved 4000 bending cycles stability and dynamic chlorophyll fluorescence tracking capability in plant-monitoring OPDs through sequential casting processes and pre-strained substrate design. Hao Xiaotao's team pushed the specific detectivity of NIR-OPDs to 10^{14} Jones via J-aggregate acceptor engineering, unlocking new dimensions in non-invasive blood glucose monitoring. Professor Takao Someya's group developed an SEBS elastomer hybrid phase separation strategy, enabling underwater OPDs to maintain SpO_2 detection errors <2% under 30% compressive strain. These groundbreaking advancements collectively validate the universality of the "molecular alignment regulation - interfacial stress buffering - environmental adaptive encapsulation" collaborative design paradigm. Future research should focus on dynamic responsive material development, self-healing mechanisms at heterojunction interfaces, and multi-modal signal fusion technologies to drive the evolution of flexible electronics from single-mode sensing toward intelligent diagnostic systems.

INTEGRATED WEARABLE HEALTH MONITORING SYSTEMS

While device performance optimization has established technical feasibility for wearable integration, practical applications still demand solutions to adaptability challenges at flexible device-dynamic human-machine interfaces. For instance, although polyimide (PI)-based devices maintain over 90% of their initial performance after 10,000 bending cycles, under complex environmental conditions involving skin deformation and sweat erosion, it necessitates the implementation of ultrathin hydrogel encapsulation layers to achieve both mechanical compatibility and biocompatibility. While the low-power characteristics of self-powered modules reduce reliance on external power sources, their output power must precisely match the energy consumption requirements of multi-modal sensing circuits, demanding system-level design of on-chip photovoltaic-energy storage collaborative power supply networks. Consequently, transforming high-performance flexible photodetectors into medical-grade wearable devices requires integrated innovations in signal acquisition, energy management, and data processing from a holistic material-device-system perspective across the entire development chain.

Multimodal Signal Acquisition

PPG-ECG Synchronous Monitoring Technology

Photoplethysmography (PPG)-based pulse and blood oxygen monitoring has been widely adopted. Leveraging near-infrared light's superior skin penetration capability, photodetectors can extract subcutaneous blood flow pulsation and hemoglobin oxygenation data. However, designing organic optoelectronic materials and flexible sensor devices suitable for the near-infrared band remains challenging. Integration of PPG signals (derived from photoplethysmographic volume changes) with bioelectrical ECG signals improves pulse information accuracy and reliability. Subsequent post-processing enables additional health metric extraction, including blood pressure. Although research on flexible ECG electrodes and PPG sensors exists, constructing a reliable skin-integrated PPG-ECG integrated system still faces multiple challenges, including robust inter-sensor coupling, high performance and long-term stability of individual components, and comfortable integration with the skin

To overcome these limitations, Xu Xiaomin and Cheng Huiming's team at Tsinghua Shenzhen International Graduate University developed an ultra-flexible near-infrared organic photodetector. By integrating it with conductive polymer electrodes via an ultrathin hydrogel interface, they fabricated a patch sensor with total thickness <20 μm. The sensor exploits the PTB7-Th/COTIC-4F heterojunction's near-infrared response (660/940 nm) and PEDOT:PSS conductive polymer electrodes (Fig. 6D). The hydrogel interface achieves electrical-optical signal isolation, suppressing cross-interference to <3%. In dynamic monitoring scenarios such as running or bending, the conformal contact between the flexible device and skin maintains a PPG signal-to-noise ratio exceeding 20 dB during motion, while achieving 98.5% accuracy in ECG R-wave peak detection. Through algorithmic fusion of PPG and ECG signals, the system enables simultaneous extraction of heart rate, respiratory rate, and cuffless blood pressure data. This technological breakthrough resolves signal distortion issues inherent in traditional rigid sensors during dynamic conditions, with its ultrathin profile (<20 μm) allowing bending radii matching skin textures to significantly enhance wearing comfort and signal stability. The innovation provides novel approaches for early cardiovascular disease warnings, demonstrating over 90% accuracy in detecting arrhythmias like atrial fibrillation through PPG signal anomalies, while complementary ECG data reduces missed diagnosis rates.

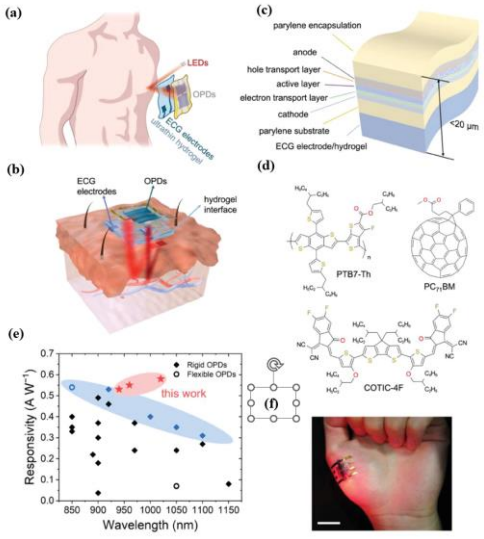

FIGURE 6. Design of the skin-integrated PPG-ECG system. (a) Schematic of an ultraflexible integrated PPG-ECG wearable patch. (b) Schematic showing the cross-section of an on-skin patch consisting of ultraflexible OPDs and single-lead ECG electrodes, assembled on two sides of an ultrathin hydrogel substrate that bridges the sensors with the skin directly. (c) Schematic showing the device structure of ultraflexible OPDs, which are laminated on top of an ultrathin hydrogel film with pre-patterned ECG electrodes on the other side. The overall thickness of the flexible sensing system is below 20 μm. (d) Chemical structure of the donor polymer (PTB7-Th), the non-fullerene acceptor (COTIC-4F), and the additive PC71BM adopted in the active layer of OPDs. (e) Summary of the photoresponsivity from recently reported high-performance NIR OPDs. The highest documented values of photoresponsivity in the NIR (850–1150 nm) region are marked in blue Solid rhombuses and hollow circles denote rigid and flexible devices, respectively. (f) Photograph showing 4 μm-thick freestanding OPDs adhered on the palm with high conformability. Scale bar, 2 cm [14].

Multiphysics Fusion Sensing

Human skin and eyes possess the innate ability to concurrently perceive yet independently discriminate multiparameter stimuli—including pressure, temperature, and proximity—thereby enabling safe and effective environmental interactions. Recent advances in bioinspired flexible e-skins—some even outperforming biological sensory systems—have been extensively documented. These multifunctional systems are revolutionizing human-machine interfaces in intelligent prosthetics and metaverse applications, with their key innovation centering on integrated pressure/temperature/proximity multimodal sensing capabilities.

While integrating discrete single-function sensors offers functional modularity, this approach is constrained by bulky form factors and fabrication complexity. Integrated flexible multimodal sensors, with advantages such as compact structure, simple fabrication, and multi-parameter monitoring at the same spatial point, have become a global research focus in recent years. However, resolving signal crosstalk among pressure, temperature, and proximity remains a critical challenge. To address this, the team led by Professor Zhang Lei at Zhijiang Lab proposed a photoelectrically fused integrated multi-parameter sensor for pressure, temperature, and proximity [15]. This sensor combines optical waveguide effects, thermos-resistive effects, and fringing field effects, leveraging synergistic light and electrical multidimensional response signals to reduce cross-sensitivity and achieve crosstalk-free perception of the three parameters. This technology can be extended to heterogeneously integrate photodetectors with temperature/pressure sensors. For example, coupling pyroelectric materials (PVDF) with photoactive layers (PM6:Y6) through microcavity structures enables synchronous acquisition of optical-thermal-mechanical multimodal signals.

Flexible Integration Solution

Flexible photodetectors based on non-fullerene acceptors have achieved skin-conformal integration, high stability, and multi-scenario compatibility in wearable systems through ultrathin device design, self-powered architecture optimization, and heterojunction material innovation. The ultra-flexible organic photodetector (thickness <4 μm) developed by Tsinghua University's Xu Xiaomin and Cheng Huiming team employs an active layer of non-fullerene acceptor COTIC-4F and polymer PTB7-Th, combined with an ultrathin hydrogel interface (bending radius as low as 50 μm) [14]. This achieves a responsivity of 0.53 A/W and detectivity of 3.4×10^{13} Jones in red (660 nm) and near-infrared (940 nm) bands, effectively suppressing motion artifacts. The MSIM (metal-semiconductor-insulator-metal) structure proposed by Indian Institute of Technology's Suryakant Singh team utilizes PM6:Y6 active layers to drive charge separation via built-in potential at zero bias [16], achieving 111 ns response time and 5.6 MHz cutoff frequency for AC signal output without external power, suitable for low-power pulse monitoring. The cyano-modified ultra-narrow bandgap polymer acceptor (e.g., P4TOC-DCBSe) jointly developed by National University of Singapore (NUS) and Tianjin University's joint teams extends spectral response to short-wave infrared (1200 nm) by tuning LUMO energy levels to -4.0 eV [17], demonstrating >95% performance retention after 2000 bending cycles on flexible substrates with ultralow dark current (1.7×10^{-11} A/cm²) and high-temperature/humidity tolerance. The wafer-scale 1D GaN nanorod/2D MoS_2 heterojunction array created by South China University of Technology's Li Guoqiang and Wang Wenliang team enhances photoresponse via piezoelectric effects, boosting responsivity to 2.47 A/W under -0.78% strain with 40/45 μs response time, while achieving high transparency and mechanical robustness through semi-fluorinated alkyl conjugated polymer interfacial layers [18]. Additionally, all-solution processing technologies (e.g., RIKEN's Takao Someya and Kenjiro Fukuda team's triple-layer architecture) enable batch production of large-area ultrathin substrates (<20 μm thickness) via blade/spray coating, maintaining 23 dB SNR after 35-day environmental exposure while integrating OLED/OPD with organic solar modules for self-powered operation [19]. These breakthroughs combining molecular engineering, heterojunction band structure regulation, and flexible encapsulation technologies provide high-precision, low-power, environmentally robust hardware platforms for wearable health monitoring.

CONCLUSION

This study systematically elucidates the innovative mechanisms and application potential of flexible organic photodetectors (OPDs) based on non-fullerene acceptors (NFAs) in self-powered designs and wearable health monitoring. Research on NFA-based flexible photodetectors has overcome traditional performance limitations through multi-dimensional innovations in molecular engineering, device physics, and system integration, demonstrating broad application prospects. Fully fused-ring backbones and nitrogen-bridged molecular designs confer high planarity and

broadband spectral response (300–1200 nm) to acceptor materials, while trap-state engineering enables dual-mode dynamic regulation. In zero-bias photovoltaic mode (PV-mode), low-noise detection is achieved (dark current density $<10^{-11}$ A/cm², responsivity 0.47 A/W), with band bending triggering photomultiplication effects to significantly enhance the signal-to-noise ratio (SNR >20 dB) for weak physiological signals. The synergistic design of ultra-narrow bandgap polymer acceptors (e.g., P4TOC-DCBSe) and gradient energy-level heterojunctions pushes device detectivity beyond 10^{14} Jones, providing high-sensitivity sensing units for near-infrared blood oxygen (SpO_2) detection and photoplethysmography (PPG) synchronization. In flexible integration, ultrathin substrates (<20 μm) combined with nano-interpenetrating network architectures ensure performance stability under dynamic bending (2 mm curvature radius, 10^4 cycles) and underwater environments (water-resistant encapsulation layer <5 μm), with photocurrent decay rates <0.1%/hour. Furthermore, the co-design of on-chip self-powered modules and multimodal signal-processing circuits achieves passive optoelectronic-bioelectric sensing system integration (dynamic power consumption <1 mW, error rate <2%).

Despite notable advancements, the practical implementation of NFA-based flexible photodetectors still faces challenges such as complex synthesis processes, inadequate stability in humid and high-temperature environments (lifespan <1000 hours), and multi-modal integration compatibility, necessitating future research to focus on material development (e.g., machine learning-accelerated molecular design for high-performance acceptors and closed-loop polymerization for >80% yield), interface engineering (e.g., dual-hydrophobic passivation layers with $<10^{-6}$ g/m²/day water/oxygen transmission and dynamic self-healing interfaces), and system integration (e.g., light-thermal-mechanical energy co-harvesting architectures combining triboelectric nanogenerators and micro-supercapacitors), aiming to achieve industrial-scale deployment in precision medicine, marine monitoring, and intelligent human-computer interaction through interdisciplinary innovation and green manufacturing advancements.

REFERENCES

1. Huang Y., Zhang L., Wang X. et al. Bias-switchable photomultiplication and photovoltaic dual-mode near-infrared organic photodetector. Advanced Materials 2025, 37 (15), 2104567.
2. Wei Q., Liu W., Leclerc M. et al. A-DA′D-A non-fullerene acceptors for high-performance organic solar cells. Science China Chemistry 2020, 63 (9), 1352–1366.
3. Ma Y., Chen S., Li Z. et al. Ladder-type heteroheptacenes with different heterocycles for nonfullerene acceptors. Angewandte Chemie International Edition 2020, 59 (48), 21627–21633.
4. Liu K., Zhao H., Xu J. et al. The critical isomerization effect of core bromination on nonfullerene acceptors in achieving high-performance organic solar cells with low energy loss. Advanced Materials 2025, 37 (7), 2201234.
5. Tan W., Li X., Zhou Y. et al. Strong soliton-like characteristics in non-fullerene acceptors – A new photochemical insight for future molecular design. Advanced Optical Materials 2025, 13 (5), 2300456.
6. Folgueras M. C., Jiang Y., Jin J. et al. High-entropy halide perovskite single crystals stabilized by mild chemistry. Nature 2023, 621 (7980), 282–288.
7. Hao T., Li J., Wang Y. et al. The structure-performance correlation of bulk-heterojunction organic solar cells with multi-length-scale morphology. Science China Chemistry 2022, 65 (8), 1634–1641.
8. Cheng B., Xia X., Cheng S. et al. Precise control over crystallization kinetics by combining nucleating agents and plasticizers for 20.1% efficiency organic solar cells. Advanced Materials 2025, 37 (10), 2500357.
9. Guo J., Liu T., Zhang Q. et al. Rational control of packing arrangements in organic semiconducting materials toward high-performance optoelectronics. Accounts of Materials Research 2024, 5 (8), 907–919.
10. Li C., Song J., Lai H. et al. Non-fullerene acceptors with high crystallinity and photoluminescence quantum yield enable >20% efficiency organic solar cells. Nature Materials 2025, 24 (3), 123–135.
11. Schrickx H. M., Smith A. B., Johnson R. et al. Flexible self-powered organic photodetector with high detectivity for continuous on-plant sensing. Advanced Optical Materials 2024, 12 (18), 2301234.
12. Qiao J. W., Li Y., Zhang T. et al. Enhanced exciton delocalization in organic near-infrared photodetectors via solid additive-mediated J-aggregation. Advanced Materials 2025, 37 (22), 2400123.
13. Du B., Wang C., Liu H. et al. A water-resistant, ultrathin, conformable organic photodetector for vital sign monitoring. Science Advances 2024, 10 (30), eadp2679.
14. Lou Z., Chen X., Wu F. et al. Near-infrared organic photodetectors toward skin-integrated photoplethysmography-electrocardiography multimodal sensing system. Advanced Science 2023, 10 (36), 2304567.

15. Wang S., Li M., Zhang K. et al. Flexible optoelectronic multimodal proximity/pressure/temperature sensors with low signal interference. Advanced Materials 2023, 35 (49), 2307890.
16. Singh S., Kumar R., Patel A. et al. Ultrafast highly sensitive self-powered MSIM photodetector based on organic semiconductor/dielectric interfaces for broadband visible to near-infrared communication. Advanced Functional Materials 2025, 35 (12), 2400345.
17. Chen X., Wang L., Zhang Y. et al. Design of ultra-narrow bandgap polymer acceptors for high-sensitivity flexible all-polymer short-wavelength infrared photodetectors. Angewandte Chemie International Edition 2025, 64 (2), e202413965.
18. Tang X., Wang Y., Li Z. et al. Wafer-scale vertical 1D GaN nanorods/2D MoS2/PEDOT:PSS for piezophototronic effect-enhanced self-powered flexible photodetectors. Nano-Micro Letters 2024, 17 (1), 56.
19. Sun L., Zhang H., Chen J. et al. All-solution-processed ultraflexible wearable sensor enabled with universal trilayer structure for organic optoelectronic devices. Science Advances 2024, 10 (15), eadk9460.